Volume 91 • Issue 2 • December 2018

Journal of Achievements in Materials and Manufacturing Engineering

International Scientific Journal published monthly by the World Academy of Materials and Manufacturing Engineering

The corrosion resistance of laser surface alloyed stainless steels

Z. Brytan

Mechanical Engineering Faculty, Institute of Engineering Materials and Biomaterials, Silesian University of Technology, ul. Konarskiego 18a, 44-100 Gliwice, Poland

Corresponding e-mail address: zbigniew.brytan@polsl.pl

ABSTRACT

Purpose: of this paper was to examine the corrosion resistance of laser surface alloyed (LSA) stainless steels using electrochemical methods in 1M NaCl solution and 1M H_2SO_4 solution. The LSA conditions and alloying powder placement strategies on the material's corrosion resistance were evaluated.

Design/methodology/approach: In the present work the sintered stainless steels of different microstructures (austenitic, ferritic and duplex) where laser surface alloyed (LSA) with elemental alloying powders (Cr, FeCr, Ni, FeNi) and hard powders (SiC, Si_3N_4) to obtain a complex steel microstructure of improved properties.

Findings: The corrosion resistance of LSA stainless steels is related to process parameters, powder placing strategy, that determines dilution rate of alloying powders and resulting steel microstructure. The duplex stainless steel microstructure formed on the surface layer of austenitic stainless steel during LSA with Cr and FeCr reveal high corrosion resistance in 1M NaCl solution. The beneficial effect on corrosion resistance was also revealed for LSA with Si_3N_4 for studied steels in both NaCl and H_2SO_4 solutions. Ferritic stainless steel alloyed with Ni, FeNi result in a complex microstructure, composed of austenite, ferrite, martensite depending on the powder dilution rate, also can improve the corrosion resistance of the LSA layer.

Research limitations/implications: The LSA process can be applied for single phase stainless steels as an easy method to improve surface properties, elimination of porosity and densification and corrosion resistance enhancement regarding as sintered material.

Practical implications: The LSA of single phase austenitic stainless steel in order to form a duplex microstructure on the surface layers result in reasonably improved corrosion performance.

Originality/value: The original LSA process of stainless steels (austenitic, ferritic and duplex) was studied regarding corrosion resistance of the alloyed layer in chloride and sulphate solutions.

Keywords: Laser surface alloying, LSA, Sintered stainless steel, Corrosion resistance, NaCl, H_2SO_4

Reference to this paper should be given in the following way:

Z. Brytan, The corrosion resistance of laser surface alloyed stainless steels, Journal of Achievements in Materials and Manufacturing Engineering 91/2 (2018) 49-59.

PROPERTIES

1. Introduction

The laser surface modification of stainless steel was widely studied for conventional grades. Whereby laser surface alloying (LSA) and melting various properties of the surface can be improved, i.e. cavitation resistance, wear resistance, corrosion resistance to pitting and intergranular corrosion attack [1-4]. The corrosion resistance of LSA stainless steel is directly related to the occurring solidification mechanism and the portion of the formed phase and the distribution of alloying elements in the microstructure. It was also reported for austenitic stainless steel that ferrite precipitations in austenitic microstructure after laser treatment were beneficial for corrosion resistance. Apart from main solidification mode it seems that a crucial factor for corrosion resistance is segregation of alloying elements between phases and morphology of formed phases influencing pit formation mechanisms.

Regarding stainless steels made by powder metallurgy, application of laser surface melting and alloying can additionally improve sintered material properties, by porosity elimination, microstructure homogenization or introduction of difficult to sintering species. One of the typical problems related to sintered stainless steels is their immune porosity and preferential corrosion attack in their presence. For this reason, sintered stainless steel shows lower corrosion performance than wrought alloys. That can be eliminated by application of laser surface treatment, like melting, alloying, cladding, etc. The one of the most promising for sintered materials seems to be laser surface alloying (LSA) with elements improving passivation of stainless steel or their compounds, like chromium, nickel, silicon and nitrogen. Moreover, different strategies of powder placing during laser treatment can be adopted giving an extended range of possible dilution rate of alloying powder and resulted microstructures of increased surface corrosion resistance. In this case, LSA with adequately balanced alloying powders (pure elements, their compounds, carbides or nitrides) can establish desired steel microstructure on the surface layer and increase corrosion resistance in corrosive media [1-7].

The LSA with austenite and ferrite former elements make it possible to form complex phase microstructure of different morphology and size in the alloyed layer of stainless steels. Alloying with ferrite former elements of austenitic stainless steel can shift primary austenitic solidification mode to primary ferritic solidification leading increase of ferrite in the microstructure. Thus, the improved corrosion resistance of resulted microstructure, saturated in alloying elements influencing passivation can be achieved. Moreover, the rapid cooling rate of laser surface treatment allows avoiding precipitation of intermetallic phases, like sigma phase, the one of most detrimental for toughness reduction and corrosion resistance deterioration of stainless steels.

The presented study derives from results described in [8-15] were sintered single phase austenitic stainless steels was laser surface alloyed (LSA) with Cr, FeCr, while ferritic stainless steel with Ni and FeNi. The LSA with ferrite and austenite former elements of the single-phase stainless steels was aimed to form a duplex (austenitic-ferritic) microstructure on the base of austenitic alloy and analyse complex microstructures deriving on the base of ferritic alloy, composed of austenite, martensite and ferrite. LSA was also aimed to increase mechanical properties of the surface layer by alloying with SiC and Si_3N_4 powders the base stainless steel material of austenite, ferritic and duplex stainless steel. The influence of LSA process parameters like laser beam power, the method of introducing alloying powder on the surface was studied. In the present study, the corrosion resistance of such LSA stainless steel was evaluated in 1M NaCl and 1M H_2SO_4 solutions by analysing the electrochemical parameters.

2. Methodology

2.1. The base material

Three types of sintered stainless steel were investigated. The austenitic stainless steel type 316L (X2CrNiMo17-12-2), ferritic 410L (X6Cr13) and duplex (X2CrNiMo22-8-2) with the composition shown in Table 1. The austenitic and ferritic alloys were sintered form commercial powder of Hoeganes with the particle size of <150 μm. The third one (duplex) was produced using 410L as starting base powder mixed with addition of alloying element powders, such as Fe-Cr, Ni and Mo in the right quantity to obtain chemical composition like duplex stainless steel – corresponding to X2CrNiMo22-8-2 acc. to EN designation system. The detailed description of the composition preparation and resulted sintered properties were described in the paper [11]. Prepared powders were then compacted at 700MPa in specimens of 10×10×55 mm and sintered in a vacuum with Ar backfilling at 1250-1260°C/60 min. During the sintering cycle a solution annealing at 1050°C/1h was done, and then the rapid cooling under pressure of 0.6 MPa of nitrogen was applied. The density of sintered stainless steel was 7.2-7.3 g/cm^3.

Table 1.
The nominal chemical composition of sintered stainless steels powders used in investigations

Powder designation	Elements concentration, wt.%								
	Cr	Ni	Mo	Si	Mn	C	N	S	Fe
316LHD (X2CrNiMo17-12-2)	16.2	12.3	2.2	0.9	0.10	0.019	0.05	0.006	bal.
410LHD (X6Cr13)	11.9	0.15	-	0.8	0.08	0.009	0.05	0.03	bal.
Duplex X2CrNiMo22-8-2	22.72	8.10	2.00	0.7	0.60	0.03	-	-	bal.

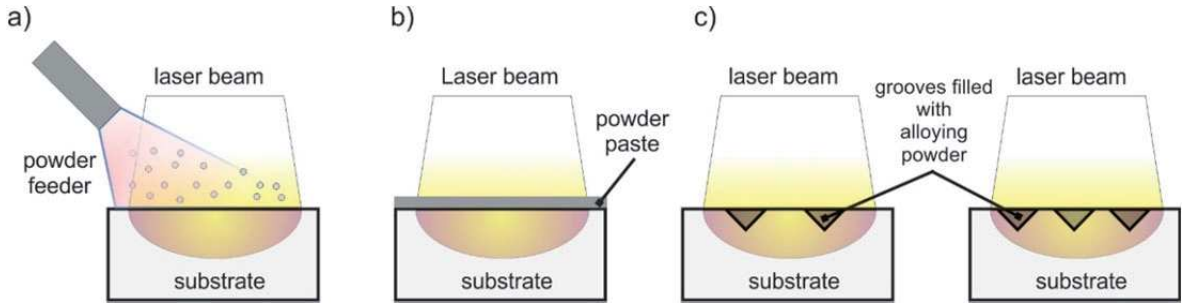

Fig. 1. Powder placement strategies during LSA of stainless steels, a) powder introduced directly to the molten metal pool by the feeder, b) powder applied as pre-coated paste, c) powder pre-placed on the surface by filling the parallel grooves machined on the sample surface

2.2. The laser surface alloying

The laser surface alloying (LSA) was done using Rofin DL 020 high power diode laser (HPDL) laser with the following laser parameters at Ar atmosphere: radiation wavelength 808±5 nm, beam output power (continuous wave) 2300 W, beam focal length 82/32 mm, rectangular laser beam spot 1.8-6.8 mm, power density range in the laser beam plane 0.8-36.5 kW/cm^2. The laser treatment was led at 0.7, 1.4 and 2.1 kW of laser beam power and constant scanning speed rate of 0.5 and 0.3 m/min.

The alloyed surface layers on sintered stainless steel were produced as single stringer beads; the laser beam was focused on the top of specimens. The long side of laser beam spot was set perpendicularly to the alloying direction. The laser beam was guided along longer side (55 mm) of specimens 10×10×55 mm, the side compatible with their pressing direction.

The surface of sintered stainless steel was alloyed with different powders: Cr, FeCr, Ni, FeNi, SiC, Si_3N_4 using different strategies: (1) the powder injected directly into the molten metal pool by the feeder, at constant powder feed rate of 5 g/min; scanning rate 0.5 m/min; (2) powder applied on the surface as pre-coated thin layer (0.1 mm) of powder paste prepared as a mixture of inorganic sodium glass in proportion 30% glass and alloying the powder; (3) the powder applied directly on the surface by filling parallel grooves (0.5 and 1.0 mm depth of a triangular shape – angle of 45°) machined on the sample surface, scanning rate 0.3 m/min. The sketch of studied different alloying powder placement strategies of LSA is presented in Figure 1.

2.3. Materials characterization

The materials microstructure was investigated by light (LOM), scanning microscopy (SEM) with the EDS analysis and correlated with the phase composition evaluated by X-Ray diffraction using filtered Cu lamp rays at 45 kV and heater current of 40 mA.

The corrosion behaviours of LSA stainless steels were evaluated by analysing the polarization curves. The testing environment was a 1M NaCl and 1M H_2SO_4 solution at room temperature. The potentiodynamic test was carried out on the Potentiostat Atlas 0531 according to PN-EN ISO 17475 standard. Test samples prior corrosion test were ground and polished to obtain flat surface of alloyed layer and uniform surface roughness. The test surface area for corrosion test was 0.2 mm^2 in the centre of top surface of alloyed zone. The silver chloride electrode (Ag/AgCl of the 0.197 V potential) was applied as the reference electrode, as the auxiliary electrode was used platinum electrode (a rod). Electrochemical studies of corrosion resistance were carried out in two steps. In the first step the open circuit potential (EOCP) after 45-60 min immersion in test solution was determined. The second stage involved the determination of anodic polarization curves by applying potential changes in the anodic and cathodic direction at a

step of 1 mV/s. The reaction of polarization curves was monitored in the range from EOCP -100 to +100 mV). On The values of corrosion potential (E_{cor}), breakdown potential (E_b), polarization resistance (R_p) and corrosion current density (i_{cor}) were determined. The corrosion current density was calculated applying the Stern-Geary equation:

$$i_{cor} = \frac{b_a \cdot b_k}{2{,}3(b_a + b_k)\boldsymbol{R_p}} \quad (1)$$

$$i_{cor} = \frac{0{,}026}{\boldsymbol{R_p}} \quad (2)$$

where: b_a and b_k – slope coefficients of the anodic Tafel's line, R_p – polarisation resistance. The coefficient of data fitting during Stern-Geary analysis was also registered (Coef).

3. Results and discussion

3.1. The microstructure of LSA stainless steel

The main microstructural phases present in the surface layer of LSA stainless steels for studied process parameters are listed in Tables 2-4. The detailed studies of presented LSA process, regarding formed phases, were previously analysed by author and presented elsewhere in works [8-15]. The laser surface alloying with ferrite and austenite former elements, supplied by alloying powders like Cr, FeCr, Ni, FeNi contribute to the microstructural changes responsible for a complex microstructure formation in the alloyed layer.

Table 2.
The LSA process parameters of austenitic stainless steel and microstructure of alloyed layer

Specimen / alloying powder		Method of LSA		Laser power P (kW)	Main phases (XRD and SEM analysis)
316L	Cr	Powder feed directly to the molten metal pool, scanning rate 0.5 m/min		0.7	Fe ɣ, Fe α
				1.4	
				2.1	
	FeCr			0.7	
				1.4	
				2.1	
	FeCr	2 / 1.0	filling parallel grooves on the surface, scanning rate 0.3m/min, quantity / grooves depth (mm)	2.1	Fe ɣ, Fe α
		3 / 0.5			
	SiC	2 / 1.0			Fe ɣ, Fe3Si, Cr5Si3, Fe2Si, C-Fe-Si, M7C3
		3 / 0.5			
	Si_3N_4	2 / 1.0			Fe ɣ
		3 / 0.5			

Table 3.
The LSA process parameters of ferritic stainless steel and microstructure of alloyed layer

Specimen / alloying powder		Method of LSA		Laser power P (kW)	Main phases (XRD and SEM analysis)
410L	Ni	Pre-coated layer (0.1) mm of powder paste		0.7	Fe ɣ
				1.4	
				2.1	
	FeNi	Powder feed directly to the molten metal pool, scanning rate 0.5 m/min		0.7	Fe ɣ, Fe α (α')
				1.4	Fe ɣ, Fe α (α')
				2.1	Fe ɣ, Fe α (α') + α'
	FeNi	2 / 1.0	filling parallel grooves on the surface, scanning rate 0.3m/min, quantity / grooves depth (mm)	2.1	Fe α + α'
		3 / 0.5			
	Si_3N_4	2 / 1.0			Fe α (α')
		3 / 0.5			
	SiC	2 / 1.0			Fe γ, Fe α (α'), Fe_3Si, Fe_2Si, C-Fe-Si and M_7C_3
		3 / 0.5			

Table 4.
The LSA process parameters of duplex stainless steel and microstructure of alloyed layer

Specimen / alloying powder		Method of LSA		Laser power P (kW)	Main phases (XRD and SEM analysis)
Duplex	Si_3N_4	2 / 1.0	filling parallel grooves on the surface, scanning rate 0.3 m/min, quantity / grooves depth (mm)	2.1	Fe ɣ + Fe α
		3 / 0.5			
	SiC	3 / 1.0			Fe ɣ + Fe α (matrix), FeSi, Fe_3Si, C-Fe-Si, M_7C_3
		3 / 0.5			

The LSA of austenitic stainless steel with ferrite former elements (in the form of Cr, FeCr) for the processing parameters results in the primary ferrite solidification mode that results in a duplex (austenite-ferrite) microstructure. When alloying with pure Cr powder, its concentration was about 28% for 1.4 and 2.1 kW of laser beam power, and a duplex (austenite-ferrite) microstructure was well formed, while lower laser beam power 0.7 kW resulted in non-fully melted powder particles embedded in the surface layer. When using FeCr powder, the higher dilution rate of alloying elements can be obtained resulting in preferential Cr/Ni ratio required to form austenite-ferrite microstructure, when high laser power of 2.1 kW was applied. Applied laser beam power (2.1 kW) supply enough heat input to the melting zone that causes the slower cooling rate, so a more significant amount of austenite can precipitate in volume. When FeCr was applied the chromium content in the alloyed layer was about 20% for 2.1 kW using powder feeding technique and filling grooves on the surface with alloying powder. Feeding FeCr powder directly to the molten metal pool during treatment at 1.4 kW of laser power resulted in higher chromium concentration ca. 28%. The same effect on chromium content (about 20%) was obtained by increasing powder volume in the grooves on the surface and alloying at 2.1 kW of laser beam power.

The ferritic stainless steel alloyed with Ni (powder feed directly to the molten metal pool – powder placing strategy (Fig. 1a) results in a fully austenitic microstructure in the alloyed zone, and in this case, a clad layer of alloying powder saturated in nickel was obtained. When alloying with pure Ni powder (applied on the surface as a pre-coated thin layer of powder paste), its content in the centre of a cross section of the alloyed layer was about 65% at 0.7kW while 45% and 33%, respectively at 1.4kW and 2.1kW of laser beam power. When using FeNi higher dilution ratio of alloying powder and the base metal was obtained resulting in austenitic phase on the top layer and the next region of mixed character austenitic-martensitic microstructure and next ferritic-martensitic one. For base metal chromium content of 13%, the falling nickel concentration contributes to austenite stability reduction along with the increase of laser beam power and leads to the formation of austenitic, mixed austenitic-martensitic and ferritic-martensitic structures. In this case, nickel content varies from approx. 40%, through 20% to 10%, respectively at a laser beam power of 0.7 kW, 1.4 kW and 2.1 kW. When filling grooves on the sample surface with FeNi and processing at 2.1 kW of laser beam power, the nickel content in the surface layer further decrees to about 5% and the alloyed layer shows the mixed ferritic-martensitic microstructure

The LSA with SiC tends to the formation of carbides and silicides depending on the dilution ratio (vary on applied process parameters) in each type of studied stainless steel. Whereas, the LSA with Si_3N_4 strongly increase the austenite content in the ferritic and duplex stainless steel. In the case of ferritic stainless steel microstructure of the alloyed layer become complex ferritic-martensitic with some austenite. In the case of duplex stainless steel, the austenite to ferrite ratio was balanced, preventing ferrite content to increase due to the rapid cooling rate during alloying.

3.2. Corrosion resistance

The corrosion resistance of laser surface alloyed (LSA) stainless steels using electrochemical methods in 1M NaCl solution and 1M H_2SO_4 solution were studied. The LSA conditions and alloying powder placement strategies on the material's corrosion resistance were evaluated. The open circuit potential (E_{OCP}), corrosion potential (E_{cor}), breakdown potential (E_{br}), polarisation resistance (R_p) and corrosion current density (i_{corr}) were determined. The coefficient of data fitting during Stern-Geary analysis was also registered (Coef).

The corrosion resistance of LSA stainless steel in 1M NaCl solution is discussed based on electrochemical parameters summarised in Figures 2-4, respectively for austenitic, ferritic and duplex base material and studied alloying powders. Polarisation curves in 1M NaCl of LSA stainless steels show stable passivation region in the anodic zone but not undergo repassivation during the reverse scan. The corrosion potential (E_{cor}) of LSA austenitic stainless steel with studied powders shows a shift to more negative

values with respect to the base material conditions, without LSA (as received). The value of corrosion current density (i_{corr}) was lower for all alloyed specimens than that of the base material. One exception is alloying with FeCr at a low laser beam power of 0.7 kW, where applied laser energy is too low to obtain fully melted material and uniform microstructure of alloyed zone. The reduction of corrosion resistance, in this case, can be explained by the presence of a large amount of not fully dissolved powder particles, which provide more interfacial area as the active sites for pitting corrosion. The LSA of austenitic stainless steel with ferrite former elements (in the form of Cr, FeCr) for the processing parameters results in the primary ferrite solidification mode that results in an austenite+ferrite microstructure. The best improvement of electrochemical parameters of LSA austenitic stainless steel was revealed, where in the surface layer a uniform microstructure of austenite+ferrite was formed. That can be seen for samples alloyed with FeCr at a laser power of 1.4 and 2.1 kW and 0.5 m/min scanning rate when powder was feed directly to the molten metal pool. Similarly, good results were evidenced for LSA samples, where the FeCr powder was fed by filling the grooves made in the surface. In this samples, the higher the polarisation resistance (R_p) and the smallest corrosion current density (i_{corr}) was registered (Fig. 2).

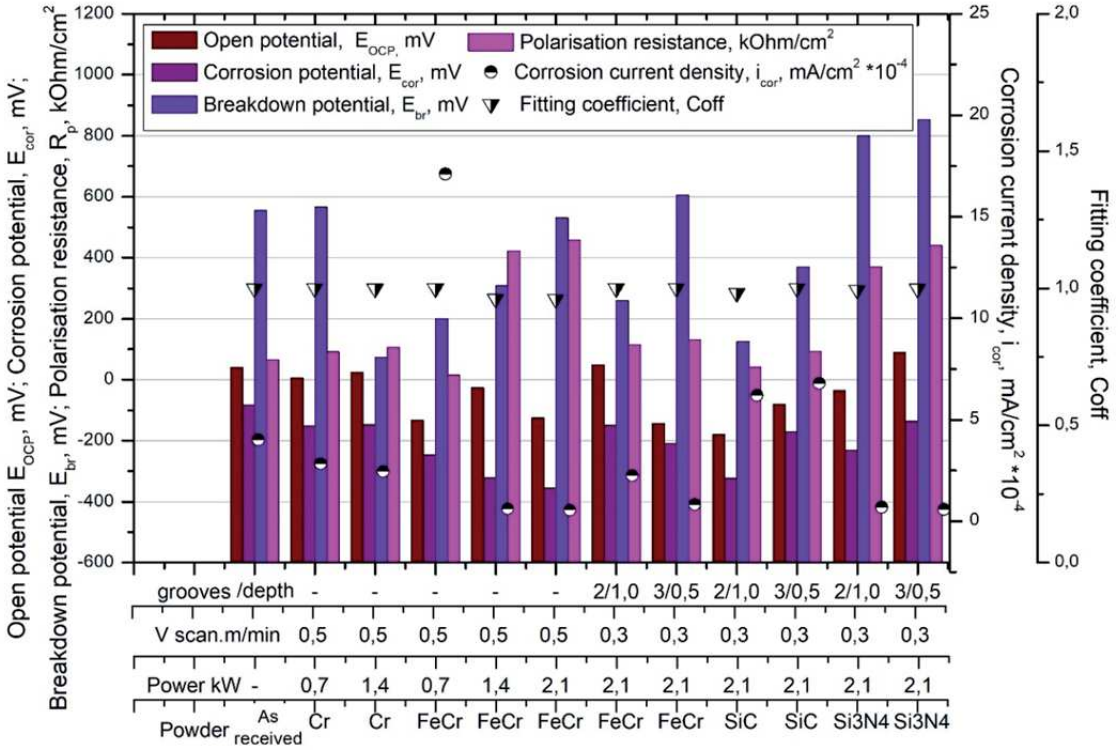

Fig. 2. The corrosion parameters of LSA austenitic stainless steel obtained from polarization data in 1M NaCl solution

LSA with SiC favours precipitation processes of secondary phases (carbides, silicides) containing a high concentration of alloying elements and zones around such precipitates depleted in alloying elements. In consequence favouring faster breakdown of the passive film. That can explain lower polarisation resistance (R_p) and breakdown potential (E_{br}) of a formed passive layer in 1M NaCl solution for SiC alloyed austenitic stainless steel.

The beneficial effect of LSA with Si_3N_4 can also be demonstrated due to the enrichment of the passive film in Si and N. Apart of alloying element segregation (silicon) between cellular grains of rapid crystallised austenitic structure the strong austenite stabilising the effect of nitrogen dissolved in the molten metal pool inhibited interdendritic ferrite precipitation. Due to nitrogen dissolution in the austenitic matrix, the alloyed layers show the broader passive range ($E_{br} - E_{cor}$) and passive layer exhibits better resistance against the development of pitting corrosion. The saturation of the steel matrix by silicon (c.a. 3% in studied cases) also was reported to be beneficial for austenitic stainless steels, improving pitting corrosion resistance due to the formation of a passive protective film rich in silicon and

chromium oxides. Additionally, such a film can reduce the adsorption of chloride ion at the interface between the solution and the metal. Besides that, such alloyed layers of austenitic stainless shows high polarisation resistance (R_p) and lower corrosion current density (i_{cor}) when compared to non-laser treated conditions (Fig. 2).

The LSA treatment of ferritic stainless steel shows improvement of electrochemical parameters (Fig. 3) regarding lower corrosion current density (icor) for Ni, FeNi and Si_3N_4 alloyed surface layers. Similarly like for austenitic alloys, alloying with SiC decrease corrosion properties due to secondary phase precipitations in the microstructure. The LSA with Ni and FeNi cause a shift of corrosion potential (E_{cor}) to more positive values in respect to the base material conditions, without LSA (as received) due to strong saturation in nickel and formation of fully austenitic clad layer when using pure Ni powder for alloying (applicated as pre-coated powder paste). Applying FeNi to LSA by filling grooves in the surface gives higher dilution rate of alloying powder (nickel content decrease from 40%, by 20% to 10% with an increase of laser beam power from 0.7 kW, by 1.4kW to 2.1 kW). Further decrees of nickel to c.a. 5% is obtained when powder was introduced on the surface by filling grooves on the sample surface and processed at 2.1 kW of laser beam power. Thus, resulted in layer microstructures changed from fully austenitic to austenitic-martensitic and at lowest nickel content to ferritic-martensitic. Regarding corrosion resistance of resulted microstructures, general improvement of electrochemical parameters for studied layers is related to higher alloying content of alloyed layer in respect to base 13%Cr ferritic stainless steel substrate. Apart of formed mixed microstructures all of them shows an increase of polarisation resistance (R_p) and breakdown potential (E_{br}) proving higher corrosion resistance of LSA layer compared to non-laser treated material. The positive effect of Si_3N_4 on the corrosion properties of LSA ferritic stainless steel is also evident and formed in this case ferritic-martensitic microstructure shows a strong increase of polarisation resistance (R_p).

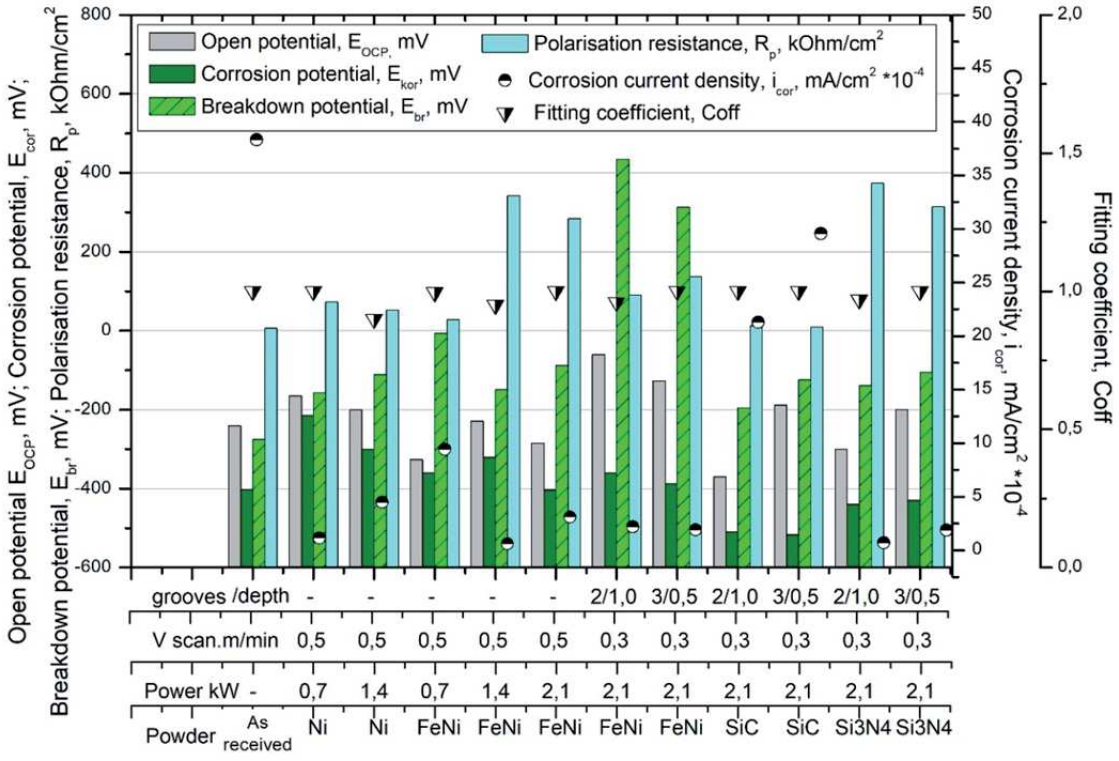

Fig. 3. The corrosion parameters of LSA ferritic stainless steel obtained from polarization data in 1M NaCl solution

When looking on the electrochemical parameters of duplex stainless steel LSA with SiC and Si_3N_4 powders the similar adverse effect of alloying with SiC and positive influence of Si_3N_4 on the corrosion resistance can be seen (Fig. 4). The fine austenitic-ferritic microstructure with acicular ferrite precipitated along primary ferritic grains and

inside ferritic grains resulted from saturation of molten metal pool by silicon and nitrogen shows higher passivation ability in the 1M NaCl solution (wider range of $E_{br} - E_{cor}$) and thus higher corrosion resistance than as-received material. The corrosion potential (E_{cor}) of Si_3N_4 LSA surface if practically the same as for non-laser treated duplex alloy, but an apparent decrease of corrosion current density (i_{cor}) and broader passive state ($E_{br} - E_{cor}$) of such processed surface is evident.

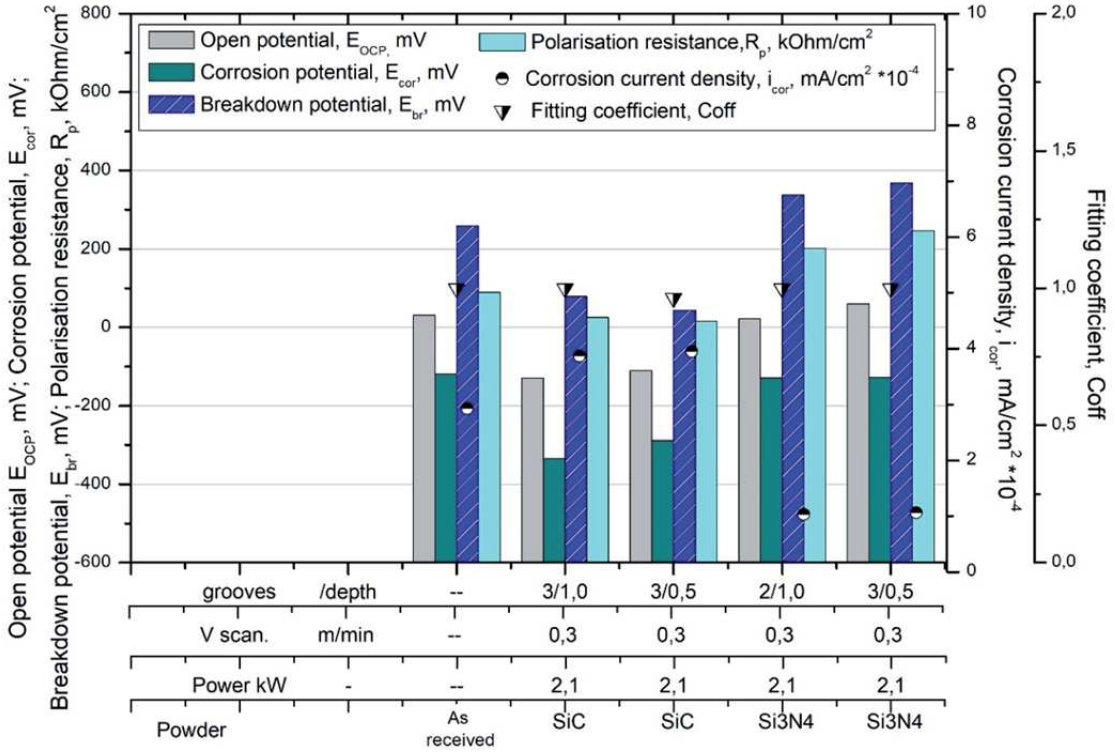

Fig. 4. The corrosion parameters of LSA duplex stainless steel obtained from polarization data in 1M NaCl solution

The corrosion resistance of LSA stainless steel in 1M H_2SO_4 solution was also studied for selected processing parameters. The electrochemical parameters resulted from polarisation scan in the 1M H_2SO_4 were summarised in Figures 5-7, respectively for LSA austenitic, ferritic and duplex base material and studied alloying powders.

The LSA stainless steel in 1M H_2SO_4 solution follows the same trends regarding corrosion resistance as for 1M NaCl. The less corrosive environment of sulphate ions results in a more positive corrosion potential (E_{cor}) of studied laser treated surface. The breakdown potential regardless of processing parameters is practically the same c.a. 1000 mV for all studied conditions. The positive effect of FeCr and Si_3N_4 during LSA of austenitic stainless steel and using FeNi and Si_3N_4 for LSA of ferritic stainless steel is also evident, while SiC alloying decrees corrosion resistance in H_2SO_4 solution (Figs. 5-7). Duplex stainless steels LSA with Si_3N_4 also shows corrosion resistance increase. The LSA cause the shift of corrosion potential (E_{cor}) to positive values and the increase of polarisation resistance (R_p) proving increased corrosion resistance of LSA stainless steel in 1M NaCl and 1M H_2SO_4 solutions.

Apart of LSA, the beneficial effect of laser treatment on the corrosion resistance of sintered stainless steel can be related to porosity elimination of the base material and removal of possible surface oxides layers in the region of porosities and sintered powder particle boundaries. The superficial oxides present on the powder parties are well known to have a detrimental effect for a proper particle bonding during sintering due to their preferential concentration in the primary porosity zones. Such oxides will also take part in the process of pitting corrosion initiation. The next issue related to the microstructure is a presence of non-metallic inclusions, like manganese sulphides acting as preferential sites for pitting initiation in stainless steels. Such inclusions will melt during laser treatment, and its constitutive elements will fully dissolve in the molten metal pool. Thus, the laser surface treatment, by melting and further alloying can eliminate such adverse effects of sintered stainless steels and improve their corrosion resistance.

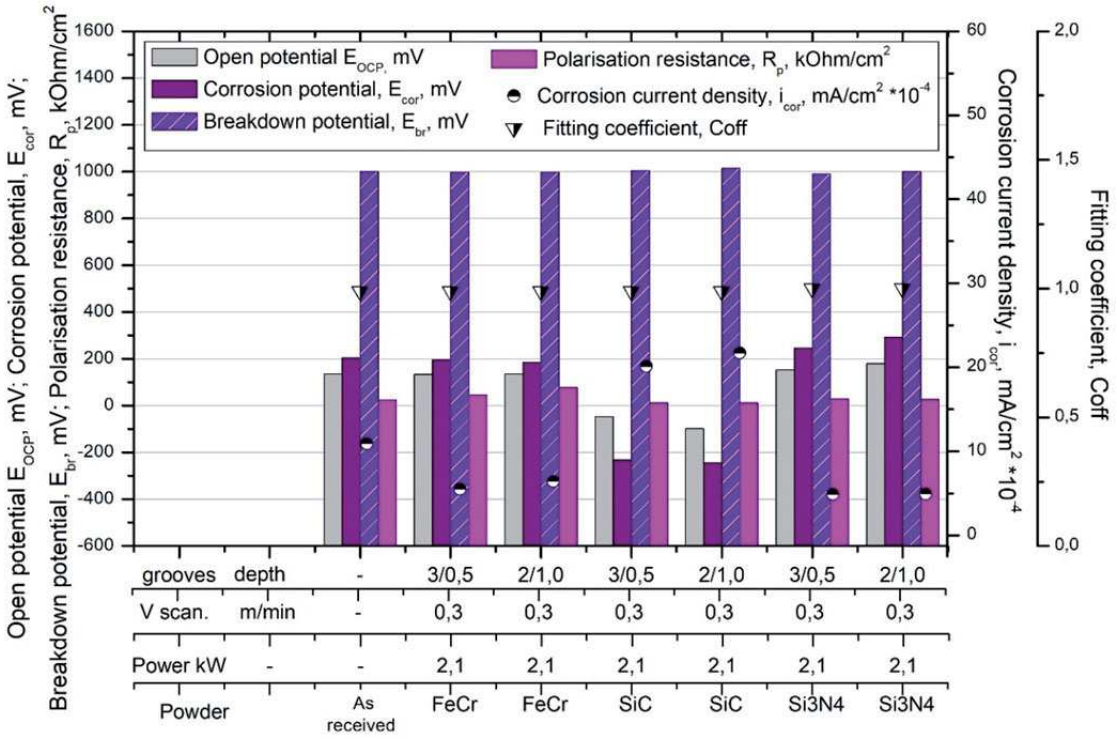

Fig. 5. The corrosion parameters of LSA austenitic stainless steel obtained from polarization data in 1M H_2SO_4 solution

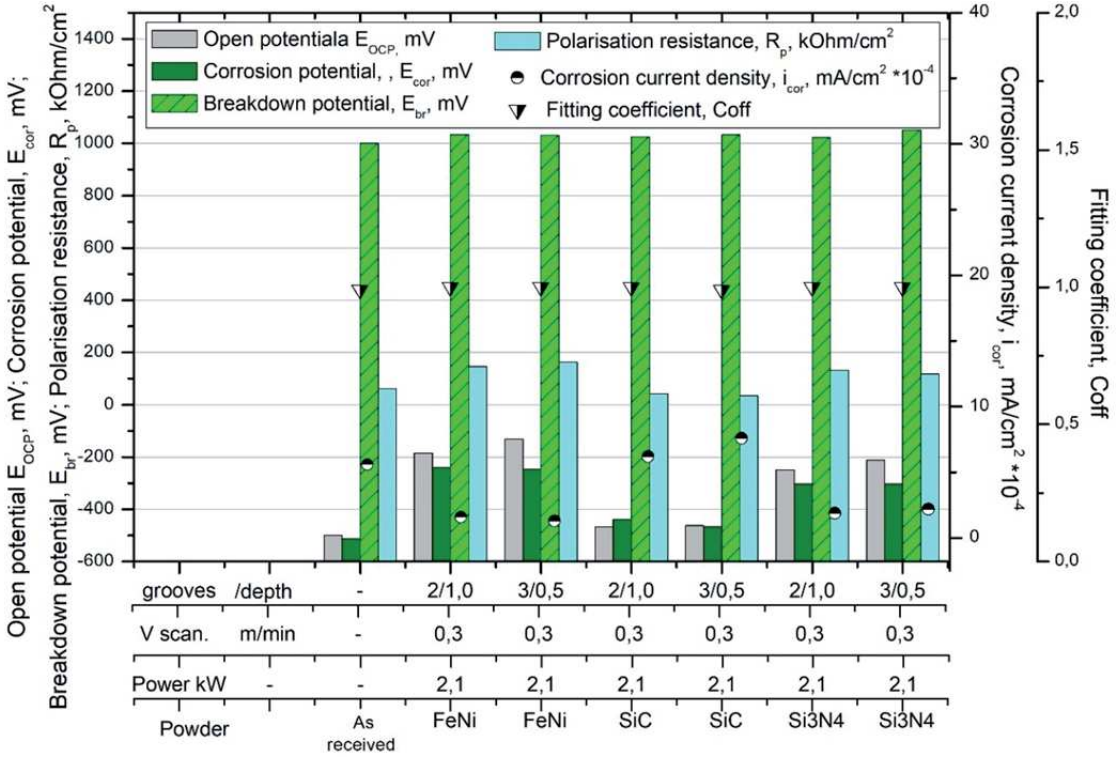

Fig. 6. The corrosion parameters of LSA ferritic stainless steel obtained from polarization data in 1M H_2SO_4 solution

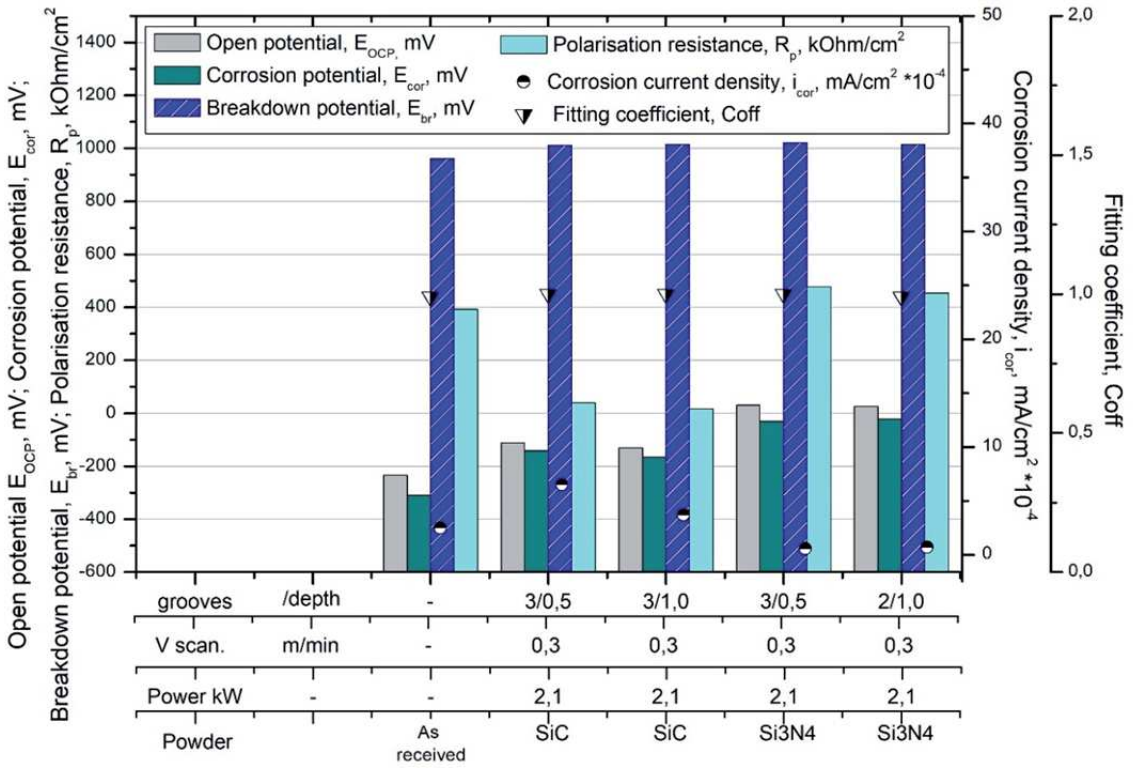

Fig. 7. The corrosion parameters of LSA duplex stainless steel obtained from polarization data in 1M H_2SO_4 solution

4. Conclusions

The corrosion resistance of laser surface alloyed sintered stainless steels in studied solutions (1M NaCl and 1M H_2SO_4) is related to different mechanisms. The first one is related to the elimination of porosity and dissolution of superficial oxides present in porosities, typical for powder metallurgy materials and homogenisation of the microstructure during laser surface treatment.

The next is related to the laser treatment involving saturation of microstructure in ferrite and austenite former elements resulting in complex phase formation during alloying and rapid cooling. The LSA of austenitic stainless steel with ferrite former elements (Cr, FeCr) results in a duplex (ferritic-austenitic) microstructure formation due to shift from primary austenite solidification mode to primary ferrite mode. The presence of duplex microstructure, together with additional saturation in chromium of steel matrix, increase the corrosion resistance of LSA stainless steel. The LSA of ferritic stainless steel with austenite former elements (Ni, FeNi) with decreasing nickel content leads to the formation of austenitic, mixed austenitic-martensitic and ferritic-martensitic microstructures in the surface layer. Saturated in nickel steel matrix despite to formation of mixed microstructures reveal improved corrosion resistance in respect to the non-laser treated ferritic stainless steel.

The beneficial effect on the corrosion resistance of LSA with Si_3N_4 was revealed for all kinds of base stainless steels alloys: austenitic, ferritic and duplex one. The strong austenite stabilisation effect of nitrogen and potential to improve the passivation mechanism of the passive layer in studied solutions resulted in increased corrosion resistance of such surface layers.

LSA with SiC favours precipitations of secondary phases (carbides, silicides) and in consequence initiation of the pitting corrosion result in a decrease of corrosion resistance of alloyed layers.

The overall effect of LSA on the corrosion resistance of stainless steel is related to alloyed layer microstructure and its saturation in alloying elements that improve passivation in tested corrosion solutions.

References

[1] C.T. Kwok, F.T. Cheng, H.C. Man, Laser surface modification of UNS S31603 stainless steel. Part I:

microstructures and corrosion characteristics, Materials Science and Engineering A 290/1-2 (2000) 55-73, DOI: https://doi.org/10.1016/S0921-5093(00)00929-1.

[2] U. Kamachi Mudali, R. Kaul, S. Ningshen, P. Ganesh, A.K. Nath, H.S. Khatak, Baldev Raj, Influence of laser surface alloying with chromium and nickel on corrosion resistance of type 304L stainless steel, Materials Science & Technology 22/10 (2006) 1185-1192, DOI: https://doi.org/10.1179/ 174328406X 118339.

[3] C. Carboni, P. Peyre, G. Beranger, C. Lemaitre, Influence of high power diode laser surface melting on the pitting corrosion resistance of type 316L stainless steel, Journal of Materials Science 37 (2002) 3715-3723, DOI: https://doi.org/10.1023/A: 1016569527098.

[4] N. Parvathavarthini, R.V. Subbarao, S. Kumar, R.K. Dayal, H.S. Khatak, Elimination of intergranular corrosion susceptibility of cold-worked and sensitized AISI 316SS by laser surface melting, Journal of Materials Engineering and Performance 10/1 (2001) 5-13, DOI: https://doi.org/10.1361/105994901770345277.

[5] A. Viswanathana, D. Sastikumar P. Rajarajan, Harish Kumar, A.K. Nath, Laser irradiation of AISI 316L stainless steel coated with Si_3N_4 and Ti, Optics and Laser Technology 39/8 (2007) 1504-1513, DOI: https://doi.org/10.1016/j.optlastec.2007.01.004.

[6] K.H. Lo, F.T. Cheng, H.C. Man, Laser transformation hardening of AISI 440C martensitic stainless steel for higher cavitation erosion resistance, Surface and Coatings Technology 173/1 (2003) 96-104, DOI: https://doi.org/10.1016/S0257-8972(03)00347-5.

[7] M.B. Lekala, J.W. van der Merwe, S.L. Pityana, Laser Surface Alloying of 316L Stainless Steel with Ru and Ni Mixtures, International Journal of Corrosion 2012 (2012) Article ID 162425, DOI: http://dx.doi.org/10.1155/2012/162425

[8] Z. Brytan, M. Bonek, L.A. Dobrzański, Microstructure and properties of laser surface alloyed PM austenitic stainless steel, Journal of Achievements in Materials and Manufacturing Engineering 40/1 (2010) 70-78.

[9] D. Zhang, X. Zhang, Laser cladding of stainless steel with Ni–Cr_3C_2 and Ni–WC for improving erosive–corrosive wear performance, Surface and Coatings Technology 190/2-3 (2005) 212-217, DOI: https://doi.org/10.1016/j.surfcoat.2004.03.018.

[10] Z. Brytan, M. Bonek, L.A. Dobrzański, W. Pakieła, Surface layer properties of sintered ferritic stainless steel remelted and alloyed with FeNi and Ni by HPDL laser, Advanced Materials Research 291-294 (2011) 1425-1428, DOI: https://doi.org/10.4028/www.scientific.net/AMR.291-294.1425.

[11] Z. Brytan, L.A. Dobrzański, W. Pakieła, Laser surface alloying of sintered stainless steels with SiC powder, Journal of Achievements in Materials and Manufacturing Engineering 47/1 (2011) 42-56.

[12] Z. Brytan, L.A. Dobrzański, W. Pakieła, Sintered stainless steel surface alloyed with Si_3N_4 powder, Archives of Materials Science and Engineering 50/1 (2011) 43-55.

[13] Z. Brytan, M. Bonek, L.A. Dobrzański, D. Ugues, M. Actis Grande, The Laser Surface Remelting of Austenitic Stainless Steel, Materials Science Forum 654-656 (2010) 2511-2514, DOI: https://doi.org/10.4028/www.scientific.net/MSF.654-656.2511.

[14] Z. Brytan, The erosion resistance and microstructure evaluation of laser surface alloyed sintered stainless steels, Archives of Metallurgy and Materials 63/4 (2018) 2039-2049, DOI: 10.24425/amm.2018.125141.

[15] Z. Brytan, T. Tański, W. Sitek, Formation of a complex two-phase duplex microstructure on the single-phase austenitic stainless steel, in: K. Świątkowski (Ed.), Polish metallurgy in 2011-2014, Committee of Metallurgy of the Polish Academy of Sciences, Akapit, Kraków, 2014, 889-904 (in Polish).